burg, *Geochim. Cosmochim. Acta* **55**, 397 (1991).
25. Rhenium and Os isotopic data were corrected for ^{17}O and ^{18}O species, and Os data were corrected for spike contributions to minor isotopes. We also corrected isotopic data for fractionation, using a $^{192}Os/^{188}Os$ ratio of 3.08271 (*14*). Under all run conditions fractionation was <1 per mil per atomic mass unit. In the isotopic analyses we used two thermal ionization mass spectrometers: a 12-inch radius of curvature, 90° sector machine at the National Institute of Standards and Technology, Gaithersburg, MD, and the 12-inch radius of curvature, 68° sector, Bobcat 1 instrument at the University of Maryland, College Park. All measurements were made with single faraday cup detectors. Signals of >1 V and >10 mV were obtained for major and minor isotopes, respectively. Each Os isotopic composition was measured on both mass spectrometers as a check on the external precision of the mass spectrometry. Each isotope ratio was measured to a 2σ (mean) precision better than 1 per mil; the ratios obtained by each mass spectrometer agreed to within ±1 per mil of the average. We determined the $^{187}Os/^{186}Os$ ratio of each sample both directly and by measuring the $^{187}Os/^{188}Os$ ratio and converting to a $^{187}Os/^{186}Os$ ratio using a $^{186}Os/^{188}Os$ ratio of 0.11990. The measured and the calculated ratios agreed to within ±1 per mil.
26. K. Ludwig, *U.S. Geol. Surv. Open File Rep. OF 88-0557* (1988).
27. J. W. Morgan, R. J. Walker, J. N. Grossman, *Lunar Planet. Sci.* **XXI**, 809 (1990).
28. R. N. Clayton, T. K. Mayeda, E. J. Olsen, M. Prinz, *Earth Planet. Sci. Lett.* **65**, 229 (1983).
29. We thank R. S. Clarke of the Smithsonian Institution for meteorite samples, the Mass Spectrometry Group of the National Institute of Standards and Technology for the use of various mass spectrometers and for donating portions of Bobcat 1, and W. A. Bowman for helping with the Bobcat 1 instrument. Discussions with S. B. Shirey were helpful. Early drafts of this manuscript benefited from the reviews of R. Brett, P. Baedecker, J. Wasson, and an unidentified reviewer. This research was partially supported by National Aeronautics and Space Administration contract 91-143.

17 October 1991; accepted 2 January 1992

Overlapping Nucleotide Determinants for Specific Aminoacylation of RNA Microhelices

CHRISTOPHER FRANCKLYN,* JIAN-PING SHI, PAUL SCHIMMEL

A seven–base pair microhelix that recapitulates a glycine transfer RNA (tRNA) acceptor helix can be specifically aminoacylated with glycine. A single base pair and the single-stranded discriminator base near the attachment site are essential for aminoacylation. These nucleotide sequence elements, and those in microhelices that can be charged with histidine and alanine, occur in the same positions and therefore overlap. Studies on a systematic set of sequence variants showed that no microhelix could be charged with more than one amino acid. Also, none of the three cognate aminoacyl-tRNA synthetases (aaRSs) gave a detectable amount of aminoacylation of the CCA trinucleotide that is common to the 3′ ends of all tRNAs, showing that the specific acceptor stem nucleotide bases confer aminoacylation. An analysis of the relative contributions of these microhelices to overall tRNA recognition indicates that their interaction with aaRSs constitutes a substantial part of the recognition of the whole tRNAs.

THE AMINO ACID ACCEPTOR STEM and the anticodon are common locations of the major determinants of aminoacylation specificity (*1, 2*). The acceptor stem is itself a substrate for alanine and histidine aaRS (*3–6*). In these cases, each respective tRNA has been shown to have its major determinant located in the acceptor stem [G3:U70 for $tRNA^{Ala}$ (*2, 3*) and the unique G−1:C73 for $tRNA^{His}$ (*6, 7*)]. These observations, the early proposal (*8*) [substantiated by recent experiments (*4, 9–12*)] that the N73 nucleotide in the acceptor stem acts in general as an important part of the system of tRNA identity elements, and the highly differentiated interactions between acceptor helix elements and synthetases that have been elucidated in the three-dimensional structures of *Escherichia coli* $tRNA^{Gln}$ (*13, 14*) and *Saccharomyces cerevisiae* $tRNA^{Asp}$ (*15*) with their respective enzymes suggest that further examples of amino acid–specific aminoacylation of acceptor stem microhelices might be found. As an additional possibility, we investigated a tRNA for which anticodon nucleotides are implicated as at least part of the tRNA identity system. Early genetic studies suggested that Gly tRNA synthetase recognizes the anticodon nucleotides C35 and C36 (*16*). However, alteration of the $tRNA^{Gly}_{CCC}$ anticodon to CUA yields an efficient Gly-inserting amber suppressor (*17*), suggesting that, for this isoacceptor, nucleotide determinants outside of the anticodon are also important for aminoacylation. The conservation of the first four acceptor stem base pairs and U73 among all three $tRNA^{Gly}$ isoacceptors (*18*) prompted us to design a set of oligonucleotide substrates with potential Gly acceptor stem determinants, both alone and in conjunction with determinants for Ala and His.

We found that a seven–base pair microhelix based on the acceptor stem sequence of $tRNA^{Gly}_{CCC}$ can be specifically aminoacylated with Gly ($micro^{Gly}$, Fig. 1A). The charging by GlyRS was less than the rate of aminoacylation of $micro^{Ala}$ and $micro^{His}$ with their cognate enzymes (*19*). The kinetic parameters for $micro^{Gly}$ aminoacylation with purified GlyRS were as follows: the Michaelis constant $K_m = 45\ \mu M$ and the rate constant $k_{cat} = 3 \times 10^{-3}\ s^{-1}$; for aminoacylation of $tRNA^{Gly}$ under similar conditions, $K_m = 0.6\ \mu M$ and $k_{cat} = 3.5\ s^{-1}$. Neither $micro^{Ala}$ nor $micro^{His}$ was aminoacylated with Gly, which suggests that although the charging of $micro^{Gly}$ by GlyRS was less efficient than the charging of microhelices by the other two aaRSs, aminoacylation of microhelices by GlyRS is sequence specific.

Because $micro^{Gly}$ retained specificity for Gly and could not be misacylated with other amino acids, we predicted that, as in the case of $micro^{Ala}$ and $micro^{His}$, aminoacylation of Gly microhelices might also be dependent on one or more sequence determinants among the nucleotides found at N73, 2:71, and 3:70. To characterize the effect of these potential determinants on each of the three aaRSs, we constructed 13 sequence variants based on a reference stem-loop sequence (Fig. 1B). In the 13 variants selected, sequences from the cognate microhelices (Fig. 2, constructs 1, 6, and 13) were grouped in different combinations to help to identify sequences necessary for Gly acceptance. Constructs 1, 6, and 13 contain the nucleotides at positions N73, 2:71, and 3:70 that are unique to the isoacceptors of $tRNA^{Ala}$, $tRNA^{His}$, and $tRNA^{Gly}$, respectively, in the context of the reference stem-loop.

As observed with the parental microhelix (Fig. 1A), there was no aminoacylation of microhelices 1, 6, and 13 with either of the other two noncognate amino acids (Fig. 3). These variants were aminoacylated by their cognate enzymes with efficiencies equal to those of their parental variants. Thus, the specificity and efficiency of aminoacylation is retained in the context of the reference structures and is largely determined by the 2:71, 3:70, and N73 nucleotides.

The 13 sequence variants were tested individually as substrates for aminoacylation by each of the three aaRSs. Each aaRS aminoacylated a unique subset of these 13 variants, and none of the variants was aminoacylated by more than one enzyme (Fig. 2). Sequence determinants in microhelices specific for GlyRS were studied with all of the constructs. The most efficient aminoacylation was achieved with the G3:C70,

Department of Biology, Massachusetts Institute of Technology, Cambridge, MA 02139.

*Present address: Department of Biochemistry, University of Vermont College of Medicine, Burlington, VT 05405.

C2:G71, U73 microhelix (microhelix 13). These nucleotides are conserved among the three $tRNA^{Gly}$ isoacceptors (*18*). A single base or base pair substitution was introduced at each of the three positions (microhelices 8 through 12). Because microhelices 8, 9, 10, and 12 lack G3:U70 and G−1:C73, they are aminoacylated with neither Ala nor His. Also, there was no detectable aminoacylation of microhelices 8, 9, and 10 with Gly, in which U73 (microhelices 8 and 9) and C2:G71 (microhelix 10), respectively, were individually changed. In contrast, G3:C70 to G3:U70 or to A3:U70 substitutions (microhelices 11 or 12) only reduced the efficiency of aminoacylation with Gly. These data suggest that both C2:G71 and U73 are required for aminoacylation with Gly.

We confirmed that previously identified primary determinants for recognition (G3:U70 for AlaRS and G−1:C73 for HisRS) are required for efficient aminoacylation in the context of the reference stem-loop. Additional sequence elements were identified that are not uniquely required for aminoacylation by AlaRS and HisRS but that do modulate charging. Thus, changes at 2:71 and 3:70 decreased but did not abolish aminoacylation by HisRS (Fig. 2, microhelices 4, 5, and 7), whereas for AlaRS, the introduction of U2:A71 substantially reduced but did not prevent aminoacylation (Fig. 2, microhelix 2).

However, when G−1:C73 was introduced, G3:U70-dependent aminoacylation with Ala was completely blocked (microhelix 4 versus microhelix 1). (A low but reproducible extent of aminoacylation was observed with a variant containing U−1:A73.) Thus, the major determinant for His identity is a blocking determinant for AlaRS that overrides the G3:U70 base pair. This result implies that aminoacylation with Ala and His is mutually exclusive. None of the Ala- or His-accepting microhelices was aminoacylated with Gly. Because C2:G71 and U73 are important for Gly acceptance, these nucleotides were introduced into Ala- and His-specific substrates. These substitutions together block aminoacylation with Ala (microhelix 11 versus 1). Because an A73 to U73 substitution reduces but does not prevent aminoacylation with Ala (*4*), we investigated the effect of C2:G71 alone (microhelix 3). The C2:G71 Gly determinant, like the G−1:C73 His determinant, blocks aminoacylation with Ala and overrides the positive G3:U70 Ala determinant (see below).

Similarly, the presence of the Gly-specific determinants U73 and C2:G71 blocks aminoacylation with His (microhelix 6 versus 13). Although U73 replaces the major His determinant G−1:C73 and is itself sufficient to prevent aminoacylation with His (microhelix 10 versus 6), the U2:A71 to C2:G71 substitution alone reduces aminoacylation efficiency (microhelix 7). Also, whereas the Gly determinants interfere with aminoacylation by HisRS and AlaRS, the converse relation also holds. Either a U73 to G−1:C73 (His determinant, microhelix 13 versus 7) or a U73 to A substitution (Ala determinant, microhelix 13 versus 8) is sufficient to prevent Gly acceptance.

The overlapping nucleotide determinants for aminoacylation of microhelices with Ala, Gly, and His are summarized in Fig. 4. The major determinants are shaded, and those that have a secondary or modulatory role [compare with (*4*)] are boxed. In general, the boxed nucleotides can be replaced with at least one alternative without elimination of aminoacylation of an oligonucleotide that has the essential major determinant or determinants for charging with a specific amino acid. The role of the G1:C72 base pair that is common to all three tRNAs has not been investigated here and thus cannot be ruled out explicitly as a contributor to the identity of any or all three of the tRNAs.

These results suggest a highly differentiated complementarity between AlaRS, GlyRS, and HisRS and the acceptor stems of their respective tRNAs. This highly specific complementarity may be in part obscured with full-length tRNAs, in which interactions outside of the acceptor stem may compensate for a less than exact fit of an acceptor helix with a particular aaRS. These considerations reflect the need for an analytical estimate of the relative contribution of the acceptor stem to the identity of the full-length tRNA molecule.

Much of the specificity of tRNA recognition occurs at the transition state of catalysis and is reflected in k_{cat} (*1, 7–12*). For AlaRS and HisRS, k_{cat} for the respective microhelix substrate is reduced to about one-twentieth of the k_{cat} for the cognate tRNA. However, for GlyRS, k_{cat} for $micro^{Gly}$ is reduced to about one-thousandth of that of the intact tRNA. This deficiency, although small in terms of activation free energy (~4.3 kcal

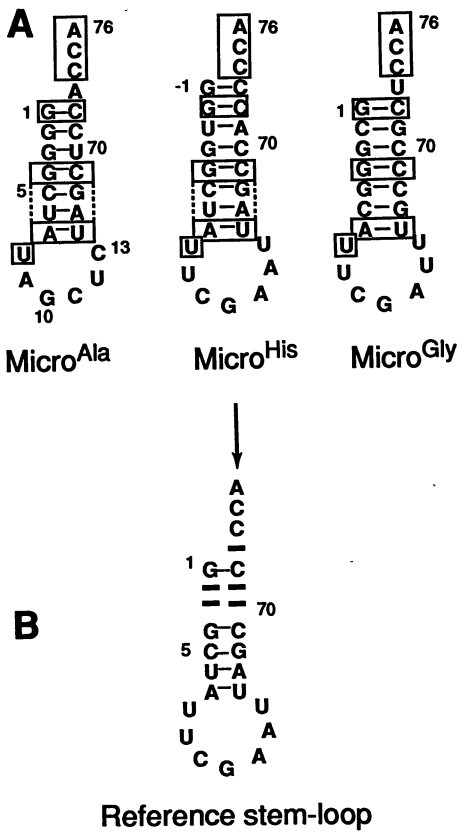

Fig. 1. Ala, His, and Gly microhelices and the derivation of the reference stem-loop sequence. (**A**) Comparison of Ala, His, and Gly microhelices that are based on the sequences of the cognate tRNAs. Nucleotides in solid boxes are common to all three sequences, and those in dashed boxes are shared by $micro^{Ala}$ and $micro^{His}$. Numbering of $micro^{Ala}$ is based on that of the full-length tRNA. (**B**) Reference stem-loop sequence. Nucleotides common to all of the microhelices used in this study are indicated. Bold dashed lines indicate nucleotides that were systematically varied. The nucleotides shared by $micro^{Ala}$ and $micro^{His}$ were used for the sequence of the lower four base pairs. Two of these base pairs (G4:C69 and A7:U66) are also shared by $micro^{Gly}$, whereas the other two (5:68 and 6:67) are not conserved among $tRNA^{Gly}$ isoacceptors. The loop sequence, which previous work had suggested is unimportant for aminoacylation of microhelices with Ala or His (*3–6*), was arbitrarily derived from the TΨC loop of $tRNA^{His}$. RNA microhelix substrates were prepared by in vitro RNA synthesis with synthetic DNA templates and purified T7 RNA polymerase (*25*). The T7 RNA polymerase used in these studies was purified from *E. coli* strain BL21/pAR1219 by the method of Grodberg and Dunn (*26*). A fivefold molar excess of guanosine 5′-monophosphate over guanosine 5′-triphosphate was included in these reactions to ensure that the transcripts initiated with 5′-monophosphates (*25*). The transcription products were purified by preparative gel electrophoresis, followed by elution of the nucleic acids from the crushed gel slices by diffusion. The RNA concentration of the preparations was determined from absorbance at 260 nm with a calculated extinction coefficient of $18.1 \times 10^4\ M^{-1}\ cm^{-1}$ (*27*). CCA was chemically synthesized on a Gene Assembler Plus Synthesizer (Pharmacia LKB, Piscataway, New Jersey) with the use of fully protected diisopropyl-β-cyanoethyl ribonucleotide phosphoramidites. The product was purified on a C_{18} high-pressure liquid chromatography (HPLC) column (VYDAC, Hesperia, California). The aaRSs were purified to near homogeneity as described (*6, 28, 29*). In general, this method consisted of cell lysis and extract clarification, Mono Q fast protein liquid chromatography, and Superose 6 or 12 chromatography (Pharmacia LKB). The active fractions identified by aminoacylation assay and sodium dodecyl sulfate–(SDS) gel electrophoresis were pooled, concentrated, and brought to 50% glycerol before storing at −20°C.

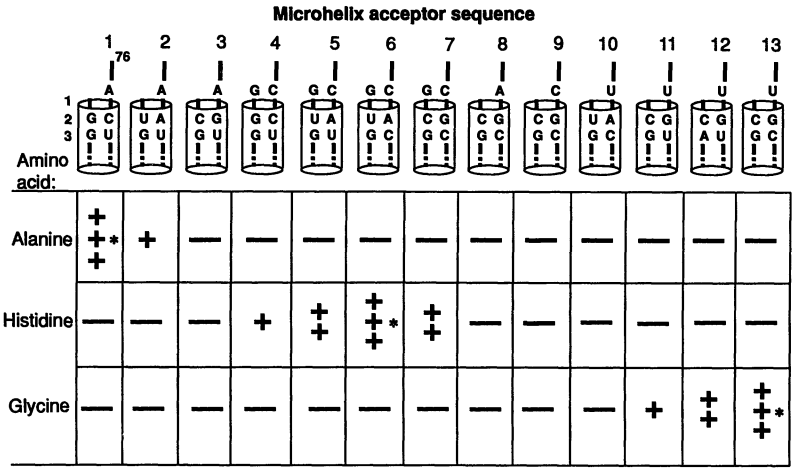

Fig. 2. Aminoacylation of microhelix sequence variants by AlaRS, HisRS, and GlyRS. The nucleotides that have been varied in each case are shown; other nucleotides in the structures are as shown in Fig. 1B. Reaction conditions were as described (*21*). Relative activities of the various substrates with the three different aaRSs are indicated by (+) and (−). Microhelices 1, 6, and 13 have the nucleotides at positions 2:71, 3:70, and 73 that are unique to the isoacceptors of $tRNA^{Ala}$, $tRNA^{His}$, and $tRNA^{Gly}$, respectively. The activity of each of these three substrates (*) is taken as the reference level (+++). In absolute terms, the rate of aminoacylation of $micro^{Gly}$ (as measured from V_{max}/K_m) is at least one-thirtieth of that of the $micro^{His}$ and $micro^{Ala}$. Each decrease of about one-tenth in the initial rate of aminoacylation (at a constant concentration of 50 μM of RNA) relative to the cognate substrate is indicated by the deletion of a plus (+). The minus (−) indicates an initial rate of incorporation $<10^{-3}$ of that of the cognate microhelix. (With the exception of variant 3, of which the rate of charging with Ala was $\sim 10^{-3}$ of $micro^{Ala}$, charging of other substrates indicated by a minus was typically equal to that of negative controls.) Each of the combinations of microhelix and aaRS was assayed at least twice.

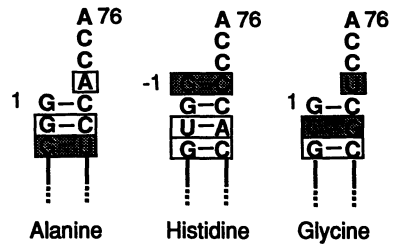

Fig. 4. Major and minor determinants for microhelix aminoacylation. Only the top portions of the acceptor stems have been shown for clarity. Determinants essential for aminoacylation by the cognate enzyme are indicated by shaded boxes. Modulating determinants are indicated by unshaded boxes.

mol^{-1}), suggests the importance of sequences outside of the acceptor stem for specific aminoacylation. The importance of sequences that are outside of the acceptor stem is reinforced by the elevated K_m values for microhelix substrates [one to two orders of magnitude larger (*3–6*)] compared to full-length tRNAs.

The operational rate of aminoacylation k (V_{max}/K_m; V_{max} = maximum velocity) is proportional to $\exp(-\Delta G^{o\dagger}/RT)$, where $\Delta G^{o\dagger}$ is the free energy of activation, R is the gas constant, and T is temperature (*20*). The lowering of $\Delta G^{o\dagger}$ by enzyme action results in rate enhancement and catalysis. The magnitude of this reduction in activation free energy ($\Delta\Delta G^{o\dagger}$) is given by $-RT\ln(k_{cat}/k_{uncat})$. Similarly, the reduction in $\Delta\Delta G^{o\dagger}$ by the enzyme interaction with a microhelix that is specifically aminoacylated versus enzymatic aminoacylation of the CCA trinucleotide (which is common to all tRNAs and microhelices) is given by $\Delta\Delta G^{o\dagger} = -RT\ln(k_{microhelix}/k_{CCA})$, and for a tRNA/microhelix comparison the relevant energy change is $\Delta\Delta G^{o\dagger} = -RT\ln(k_{tRNA}/k_{microhelix})$. Relative kinetic parameters (expressed as $k_{mutant}/k_{wild\text{-}type}$) have been used in the comparison of mutant versus wild-type tRNA sequences (*1, 7, 9, 10*).

The relative contribution of the acceptor stem to tRNA recognition is difficult to analyze because highly sensitive measurements of the aminoacylation of adenosine or of the CCA trinucleotide that is common to the 3′ ends of tRNAs are not available, nor are there data on the uncatalyzed chemical aminoacylations of the 3′ ends of RNAs by amino acids and adenosine triphosphate (ATP) or by the aminoacyl-adenylates. In an attempt to assess these rates, we measured the aminoacylation of CCA (at a concentration of 1 mM) by relatively high concentrations (6 to 10 μM) of AlaRS, HisRS, or GlyRS in separate reactions that included the respective cognate amino acid and ATP (Fig. 5). These experiments were designed to detect 5 ppm of aminoacylated CCA. Control experiments established that each enzyme retained >90% of its activity throughout the incubation and that CCA trinucleotide remained intact. In all cases, no aminoacylation could be detected after 1 hour.

From this result, we estimated that at 10 μM AlaRS or HisRS and 6.6 μM GlyRS, $k_{CCA} < 1.4 \times 10^{-9}$ s^{-1} (*21*). Values for k_{tRNA} and k_{micro} for each of these amino acid systems can be computed from published values and from this work (*3–6, 22*). The relative kinetic parameters k_{tRNA}/k_{micro} and k_{micro}/k_{CCA} and the associated reductions in activation free energy contributed by each part of the tRNA are listed in Table 1. The ratio of k_{tRNA}/k_{CCA} is greater than 10^9 to 10^{10} in each of these cases and establishes the dynamic range of the system. For $tRNA^{Ala}$ and $tRNA^{His}$, the major contribution to the V_{max}/K_m parameter for recognition is the acceptor helix. For $tRNA^{Gly}$, the recognition of the acceptor helix also makes the largest contribution to the reduction in $\Delta\Delta G^{o\dagger}$ relative to the full tRNA, but less so than that of the other two microhelices.

The demonstration of specific aminoacylation of microhelix structures with Gly is particularly significant because of the genetic evidence for a role of the anticodon in discrimination of $tRNA^{Gly}$ (*16*). The aminoacylation of microhelices suggests that interactions with the acceptor stem itself are sufficient to form a viable transition state for

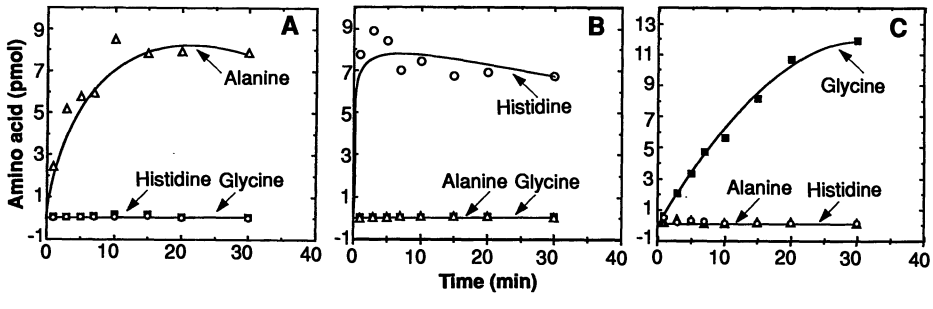

Fig. 3. Aminoacylation of Ala, His, and Gly reference stem-loop microhelices by cognate and noncognate *E. coli* aaRSs at pH 7.5 and 37°C (RNA substrates, 50 μM; aaRSs, 1 μM). (**A**) AlaRS, (**B**) HisRS, and (**C**) GlyRS. The arrows denote the extent of aminoacylation of the various microhelices. Data from two independent assays of the reference stem-loop $micro^{Gly}$. Similar data were obtained both with the parental microhelix sequences (Fig. 1A) and the reference stem-loop sequences. The incorporation of amino acid per 6-μl reaction aliquot is given on the ordinate axis.

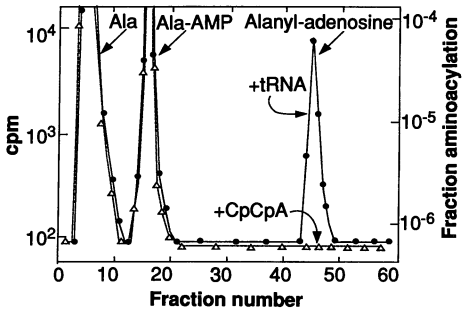

Fig. 5. Elution profile of alanyl-adenosine and estimation of fractional aminoacylation. The detection sensitivity for alanyl-adenosine is expressed as the fraction aminoacylation, defined as the fraction of 1 mM RNA substrates (tRNA or CCA) that gave alanyl-adenosine. Aminoacylation of CCA was carried out at 37°C for 1 hour in 50 mM phosphate buffer (pH 7.5) containing ^{3}H-labeled amino acid, 2 mM ATP, 1 mM CCA, 10 mM $MgCl_2$, 20 mM KCl, and substrate amounts of aaRSs (10 μM AlaRS or HisRS, and 6.7 μM GlyRS). The aminoacylated reaction products were digested with ribonuclease A (Boehringer Mannheim) for 10 min at 37°C at an enzyme to substrate molar ratio of 1:25. The digestion was stopped by addition of 3.5 M acetic acid. After centrifugation to remove protein, the hydrolysate was analyzed on a VYDAC 401 HPLC column with a linear gradient from 50 mM to 1 M sodium acetate (pH 5.2). In the case of the His system, the gradient was followed by an elution with 3 M sodium acetate (pH 5.2) in order to elute histidinyl-adenosine from the column. Fractions (1 ml) were collected and counted with Hydrofluor (National Diagnostics, Manville, New Jersey). The elution profile of each ^{3}H-labeled aminoacyl-adenosine was obtained by digestion and chromatography of the appropriate aminoacylated tRNA, under the conditions described above. A minute amount of ribonuclease A–digested aminoacyl-tRNA (to produce aminoacyl-adenosine) was loaded on to the column to calibrate the sensitivity of the system. From this standard, we concluded that this system can detect a fractional extent of the aminoacylation of 5 nM CCA that is equal to 5×10^{-6} of the starting concentration (*21*). At the end of each reaction with CCA, control reactions were carried out to confirm that the remaining amino acid and ATP were utilizable upon addition of fresh cognate tRNA and enzyme. In another set of control reactions, the extent of enzyme activity remaining in each of the three reactions was measured and found to be at least 90% of the starting activity. The stability of CCA remaining after incubation was determined from thin layer chromatography with either 1 M sodium acetate (pH 5.2) or 1 M lithium chloride–1 M formic acid as solvent systems.

Table 1. Relative contribution to the recognition parameter k (V_{max}/K_m) of the microhelix acceptor stem versus the rest of tRNA structure. Free energy values pertain to 37°C.

Parameters	Relative k	$-\Delta\Delta G^{\circ\dagger}$ (kcal mol^{-1})
	Alanine	
k_{tRNA}/k_{CCA}	$>1.4 \times 10^9$	>12.9
k_{micro}/k_{CCA}	$>1.0 \times 10^6$	>8.5
k_{tRNA}/k_{micro}	1.4×10^3	4.4
	Histidine	
k_{tRNA}/k_{CCA}	$>1.6 \times 10^{10}$	>14.4
k_{micro}/k_{CCA}	$>8.6 \times 10^7$	>11.2
k_{tRNA}/k_{micro}	1.9×10^2	3.2
	Glycine	
k_{tRNA}/k_{CCA}	$>2.7 \times 10^{10}$	>14.7
k_{micro}/k_{CCA}	$>3.0 \times 10^5$	>7.7
k_{tRNA}/k_{micro}	9.5×10^4	7.0

catalysis. The failure to aminoacylate the CCA trinucleotide and the high specificity observed in the experiments with microhelix sequence variants (Fig. 2) emphasize the role of specific sequence elements in the charging of RNA oligonucleotides. The exclusive aminoacylation with one amino acid of an RNA that has two major determinants is well illustrated by the blocking of a G3:U70-containing substrate by the histidine G−1:C73 determinant. Without more structural information, it is not possible to predict why one determinant (G−1:C73) and not the other (G3:U70) is dominant. The microhelix substrates reveal only properties of the acceptor helix–aaRS complementarity, and other parts of a tRNA may add to or subtract from the contribution to the $\Delta G^{\circ\dagger}$ that is made by the acceptor helix.

The overlapping nucleotide determinants for each of the three microhelices include the span in the acceptor helix from N73 to base 3:70 (Fig. 4). The importance of bases within this span is evident in genetic and biochemical studies of tRNA^{Ala} (*2, 3*), tRNA^{Gln} (*10*), and tRNA^{Ser} (*1, 11*), and in the cocrystals of *E. coli* tRNA^{Gln} (*13*) and *S. cerevisiae* tRNA^{Asp} (*15*), with their respective aaRSs. The cocrystal studies reveal the significance of interactions between the synthetases and the ends of acceptor stems but also show that parts of the tRNA outside of the acceptor stem (such as the anticodon) have substantial interactions with the proteins (*14*). An analysis of microhelix substrates in these systems would help to clarify the relative role of adaptation of the aaRSs to a specific acceptor sequence or structure that is evident in these cocrystals. Nucleotides at the end of the acceptor stem also appear to be important for the discrimination of elongator and initiator tRNAs and, therefore, may be critical for interactions with proteins other than aaRSs (*23, 24*).

REFERENCES AND NOTES

1. P. Schimmel, *Biochemistry* **28**, 2747 (1989); J. Normanly and J. Abelson, *Annu. Rev. Biochem.* **58**, 1029 (1989); L. H. Schulman and H. Pelka, *Nucleic Acids Res.* **18**, 285 (1990); *Science* **246**, 1595 (1989); T. Muramatsu *et al.*, *Nature* **336**, 179 (1988).
2. Y.-M. Hou and P. Schimmel, *Nature* **333**, 140 (1988); W. H. McClain and K. Foss, *Science* **240**, 793 (1988).
3. C. Francklyn and P. Schimmel, *Nature* **337**, 478 (1989).
4. J.-P. Shi, C. Francklyn, K. Hill, P. Schimmel, *Biochemistry* **29**, 3621 (1989).
5. K. Musier-Forsyth *et al.*, *Proc. Natl. Acad. Sci. U.S.A.* **88**, 209 (1991).
6. C. Francklyn and P. Schimmel, *ibid.* **87**, 8655 (1990).
7. H. Himeno *et al.*, *Nucleic Acids Res.* **17**, 7855 (1989).
8. D. M. Crothers, T. Seno, D. Soll, *Proc. Natl. Acad. Sci. U.S.A.* **69**, 3063 (1972).
9. J. R. Sampson, A. B. DiRenzo, L. S. Behlen, O. C. Uhlenbeck, *Science* **243**, 1363 (1989); J. Pütz, J. D. Puglisi, C. Florentz, R. Giegé, *ibid.* **252**, 1696 (1991); T. Hasegawa *et al.*, *Biochem. Biophys. Res. Commun.* **163**, 1534 (1989).
10. M. Jahn, M. J. Rogers, D. Söll, *Nature* **352**, 258 (1991); M. J. Rogers and D. Söll, *Proc. Natl. Acad. Sci. U.S.A.* **85**, 6627 (1988).
11. H. Himeno *et al.*, *Nucleic Acids Res.* **18**, 6815 (1991).
12. S. J. Park, Y.-M. Hou, P. Schimmel, *Biochemistry* **28**, 2740 (1989); J. P. Shi and P. Schimmel, *J. Biol. Chem.* **266**, 2705 (1991).
13. M. A. Rould, J. J. Perona, D. Söll, T. A. Steitz, *Science* **246**, 1135 (1989).
14. M. Rould *et al.*, *Nature* **352**, 213 (1991).
15. M. Ruff *et al.*, *Science* **252**, 1682 (1991).
16. J. Carbon and E. W. Fleck, *J. Mol. Biol.* **85**, 271 (1974); J. Carbon and J. W. Roberts, *Nature* **250**, 412 (1974).
17. J. Normanly, L. G. Kleina, J.-M. Masson, J. Abelson, J. H. Miller, *J. Mol. Biol.* **213**, 719 (1990).
18. M. Sprinzl *et al.*, *Nucleic Acids Res.* **17**, r1 (1989); W. H. McClain *et al.*, *Proc. Natl. Acad. Sci. U.S.A.* **88**, 6147 (1991).
19. Aminoacylation assays were carried out with a modification of described methods (*3–6*). This modification was necessary to study the charging of weakly aminoacylated substrates (such as micro^{Gly}) that were charged less efficiently than their micro^{Ala} or micro^{His} counterparts. For maximum sensitivity, the concentrations of RNAs, amino acids, and aaRSs were altered. Thus, ^{3}H-labeled amino acids were used without mixing with unlabeled amino acids to give final concentrations of 2.32 μM (Ala), 2.44 μM (His), and 1.96 μM (Gly) in the aminoacylation reactions featuring the respective aaRSs. For those reactions in which aminoacylation was determined qualitatively, concentrations of RNA and aaRSs were typically held fixed at 50 μM and 0.75 to 1.5 μM, respectively. Kinetic parameters for the aminoacylation of micro^{Gly} were obtained from duplicate initial rates over an RNA concentration range of 10 to 100 μM, with a concentration of GlyRS of 1 μM. In previous work (*3–6*), we assumed that ^{3}H in the form of free amino acid molecules is quantitated identically as trichloroacetic acid precipitation of aminoacylated RNA molecules. We have since observed differential quenching in typical organic scintillants of free ^{3}H-labeled amino acid and aminoacylated RNA molecules precipitated on Whatman 3 MM pads. The differential quenching was not observed with ^{14}C-labeled amino acids. Thus, correction factors for tRNA^{Ala} and tRNA^{His} and mini- and microhelix substrates were obtained by determination of the ratio of ^{14}C/^{3}H at the plateau phase of aminoacylation. Unlike micro^{Ala} and micro^{His}, micro^{Gly} was not quantitatively aminoacylated within the 2-hour time frame of a typical aminoacylation reaction. Thus, the correction factor for micro^{Gly} was derived from the ratio of the initial rates of aminoacylation with ^{14}C- and ^{3}H-labeled Gly.
20. G. C. Hammes, *Enzyme Catalysis and Regulation* (Academic Press, New York, 1982), p. 76; A. Fersht, *Enzyme Structure and Mechanism* (Freeman, San Francisco, 1977), pp. 33–35.
21. Under the conditions used to measure the rate of aminoacylation of CCA (1 mM trinucleotide and ~10 μM aaRS) the specific activity of ^{3}H-labeled amino acid (for example, alanine) was 7500 cpm pmol^{-1}. If k_{CCA} were equal to 1.4×10^{-9} s^{-1}, then 0.1 pmol of ^{3}H-labeled Ala, detected as 750 cpm, would have been produced over the course of a 1-hour reaction in a 20-μl reaction volume. This value is more than six times as large as the background (<100 cpm) observed in the control with no RNA.

22. We obtained the apparent kinetic parameters used in these calculations as described (*3–6*), taking into account the technical issues associated with the differential quenching of ^{3}H-labeled amino acids (*19*). We obtained the micro^{Ala} and micro^{His} kinetic parameters by measuring the initial rates of aminoacylation of microhelices over a greater concentration range than that used in previous work (1 to 500 μM versus 1 to 50 μM [RNA]), and this gives a lower apparent V_{max}/K_m for micro^{Ala} (Table 1) than reported (*3*). The k_{cat} parameter may vary with the degree of saturation of the tetrameric AlaRS.
23. B. L. Seong, C. P. Lee, U. L. RajBhandary, *J. Biol. Chem.* **264**, 6508 (1989).
24. Recently, the aminoacylation with methionine of small RNA helices based on the acceptor stem of initiator and elongator tRNA^{Met} has been observed [S. A. Martinis and P. Schimmel, *Proc. Natl. Acad. Sci. U.S.A.* **89**, 65 (1992)].
25. J. F. Milligan and O. C. Uhlenbeck, *Methods Enzymol.* **180**, 51 (1989).
26. J. D. Grodberg and J. J. Dunn, *J. Bacteriol.* **170**, 1245 (1988).
27. J. D. Puglisi and I. Tinoco, Jr., *Methods Enzymol.* **180**, 304 (1989).
28. K. Hill and P. Schimmel, *Biochemistry* **28**, 2577 (1989).
29. M. J. Toth and P. Schimmel, *J. Biol. Chem.* **265**, 1005 (1990).
30. We thank N. Usman for preparing the CCA trinucleotide and M. Davis for the gift of *E. coli* AlaRS. We thank M. Saks, J. Sampson, W. T. Miller, K. Musier-Forsyth, J. Burbaum, U. L. RajBhandary, and D. Söll for their comments on the manuscript. Supported by NIH grant 15539. C.F. was an NIH postdoctoral fellow.

5 September 1991; accepted 20 December 1991

Specific Acceptance of Cardiac Allograft After Treatment with Antibodies to ICAM-1 and LFA-1

MITSUAKI ISOBE,* HIDEO YAGITA, KO OKUMURA, AKIRA IHARA

An indefinite survival of cardiac allografts between fully incompatible mice strains was observed when monoclonal antibodies (MAbs) to intercellular adhesion molecule–1 (ICAM-1) and leukocyte function–associated antigen-1 (LFA-1) were simultaneously administered after the transplantation for 6 days. Mice with long-term surviving cardiac allografts accepted skin grafts from the donor-strain but rejected skin grafts from a third-party strain. Because MAbs to ICAM-1 or LFA-1 alone were insufficient for prolonged tolerance, the two MAbs probably acted synergistically to induce specific unresponsiveness. Thus, ICAM-1–LFA-1 adhesion participates in the induction of allograft rejection and MAbs may be useful as therapeutic agents.

ADHESION MOLECULES PARTICIPATE in the many stages of an immune response (*1, 2*). T cell immune recognition requires the contribution of the T cell receptor as well as adhesion receptors, which promote attachment of T cells to antigen-presenting cells (APCs) and transduce regulatory signals for T cell activation. The LFA-1 and ICAM-1 adhesion molecules form one such heterophilic receptor-ligand pair (*3, 4*). LFA-1 is required for a range of leukocyte functions, including lymphokine production of helper T cells in response to APCs, killer T cell–mediated target cell lysis, and immunoglobulin (Ig) production through T cell–B cell interactions (*2, 5*). Activation of antigen receptors on T cells (*2*) and B cells (*6*) allows LFA-1 to bind its ligand with higher affinity. Also, the LFA-1–ICAM-1 interaction is required for optimizing T cell function in vitro (*7, 8*). Therefore, MAbs to these molecules are potential agents for the prevention of graft rejection (*9*). In this report, we demonstrate the effect of the combination of these two MAbs on allograft survival, which leads to specific tolerance in a mouse heterotopic cardiac allograft model.

The MAbs used in this study, KBA (IgG2a) (*10*), M18/2 (IgG2a) (*11*), and YN1/1.7 (IgG2b) (*12, 13*) are rat MAb to mouse CD11a (α chain of LFA-1), CD18 (β chain of LFA-1), and ICAM-1, respectively (*14*). Because M18/2 does not block cell-mediated target cell lysis in vitro (nonneutralizing MAb) (*11*), we used M18/2 as control MAb. Hybridoma cells that produce these MAbs were cultured in RPMI 1640 supplemented with 10% fetal bovine serum and 0.1% gentamycin. The MAbs from ascites produced in nude mice were purified with the use of a protein G affinity column.

BALB/c (H-2^d) hearts were heterotopically transplanted into C3H/He (H-2^k) recipients by a microsurgery technique (*15, 16*). Survival of cardiac grafts was assessed by daily palpation, and the cessation of graft beat was interpreted as the completion of rejection (*16*). Because of the full incompatibility of the H-2 complex, control C3H/He mice without any treatment invariably rejected BALB/c heart allografts within 10 days (Table 1). Treatment of recipient mice with M18/2 did not prolong allograft survival. Animals treated with daily doses of 100 μg of either YN1/1.7 or KBA showed significant prolongation of allograft survival when compared to the control or M18/2-treated mice. However, all these animals rejected allografts within 50 days. In contrast, all nine animals treated with 50 μg of YN1/1.7 together with 50 μg of KBA accepted cardiac allografts as long as the observation was continued (75 to 200 days). The intensity and frequency of beating of these allografts were indistinguishable from those of isografts.

Histological examination of the grafts treated with the two MAbs showed greatly reduced mononuclear cell infiltration at the seventh day as compared with control allografts without treatment (Fig. 1, A and B). The treated allografts removed at 40, 75 (Fig. 1C), and 120 days after operation showed only scattered areas of fibrosis without any evidence of active rejection.

Cytotoxic T lymphocyte (CTL) activity of

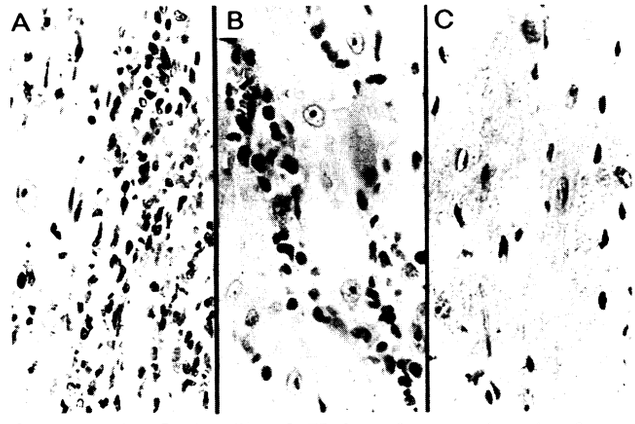

Fig. 1. Histological analysis of BALB/c heart allografted in C3H/He recipient. (**A**) A control allograft 7 days after the transplantation with no immunosuppressive treatment. Massive infiltration of leukocytes together with myocyte necrosis and interstitial hemorrhage are noted. (**B**) An allograft 7 days after transplantation from a mouse that was treated with a 6-day course of YN1/1.7 and KBA MAb commencing immediately after the transplantation. Diffuse interstitial infiltrates are noted, but the myocytes are free from necrosis. (**C**) An allograft 75 days after transplantation from a recipient that was treated as in (B). No sign of active rejection is seen. All sections are fixed in 10% formalin and stained with hematoxylin-eosin. Original magnification is ×200.

M. Isobe, Cardiac Unit, Jackson 14, Massachusetts General Hospital, Boston, MA 02114 and Harvard Medical School, Boston, MA 02115.
H. Yagita and K. Okumura, Department of Immunology, Juntendo University School of Medicine, Tokyo, 113, Japan.
A. Ihara, Pathology Research Laboratory, Massachusetts General Hospital-East, Charlestown, MA 02129.

*To whom correspondence should be addressed. Present address: The Third Department of Internal Medicine, University of Tokyo, Hongo, Bunkyo-Ku, Tokyo, 113, Japan.